George, S. S., M. N. Shivdasani, and J. B. Fallon. 2016. Effect of current focusing on the sensitivity of inferior colliculus neurons to amplitude-modulated stimulation. *Journal of Neurophysiology*. **116**: 1104-16.

Effect of current focusing on the sensitivity of inferior colliculus neurons to amplitude modulated stimulation

Shefin S. George[1,2], **Mohit N. Shivdasani**[1,2,*] **and James B. Fallon**[1,2,*]

[1] The Bionics Institute, East Melbourne, Australia, 3002

[2] Department of Medical Bionics, University of Melbourne, Melbourne, Australia, 3002

[*] These authors contributed equally to this work

Running Head: Modulation sensitivity of current focusing strategies

Correspondence: A/Prof James Fallon, The Bionics Institute, 384-388 Albert Street, East Melbourne, Victoria 3002, Australia, Phone: +61 3 9667 7576; jfallon@bionicsinstitute.org

ABSTRACT

In multichannel cochlear implants (CIs), current is delivered to specific electrodes along the cochlea in the form of amplitude-modulated pulse trains, to convey temporal and spectral cues. Our previous studies have shown that focused multipolar (FMP) and tripolar (TP) stimulation produce more restricted neural activation and reduced channel interactions in the inferior colliculus (IC), compared to traditional monopolar (MP) stimulation, suggesting that focusing of stimulation could produce better transmission of spectral information. The present study explored the capability of IC neurons to detect modulated CI stimulation with FMP and TP stimulation, compared to MP stimulation. The study examined multiunit responses of IC neurons in acutely deafened guinea pigs by systematically varying the stimulation configuration, modulation depth and stimulation level. Stimuli were sinusoidal amplitude-modulated pulse trains (carrier rate of 120 pulses/sec). Modulation sensitivity was quantified by measuring modulation detection thresholds (MDTs), defined as the lowest modulation depth required to differentiate the response of a modulated stimulus from an unmodulated one. While MP stimulation showed significantly lower MDTs than FMP and TP stimulation (*p*-values<0.05) at stimulation ≤ 2 dB above threshold, all stimulation configurations were

found to have similar modulation sensitivities at 4 dB above threshold. There was no difference found in modulation sensitivity between FMP and TP stimulation. The present study demonstrates that current focusing techniques such as FMP and TP can adequately convey amplitude modulation, and are comparable to MP stimulation especially at higher stimulation levels, although there may be some trade-off between spectral and temporal fidelity with current focusing stimulation.

Keywords

Cochlear implant; Multipolar Stimulation; Current focusing; Modulation detection; Inferior colliculus

INTRODUCTION

Along with improved speech processor hardware and electrode designs, developments in stimulation strategies, such as the use of amplitude-modulated interleaved electrical pulse trains, have resulted in remarkable speech understanding in multichannel cochlear implant (CI) users (Wilson et al., 1991, McDermott et al., 1992, Dorman, 1993, Skinner et al., 1994). In most modern stimulation strategies, the slow varying temporal envelopes of band-pass filtered components of sound are conveyed in the modulation waveforms and the spectral information is transmitted by activation of electrodes at appropriate cochlear places. The electrodes are stimulated typically in a monopolar (MP) configuration, where stimuli are presented to single intracochlear electrodes with reference to a remote extra-cochlear electrode. In contrast to the generally good speech comprehension in most CI users in quiet conditions, there is a great deal of difficulty when speech is presented in noise (Fu et al., 1998). Many patients report poor perception of sounds such as music and tonal languages that are rich in temporal and spectral information (Skinner et al., 1994, Sucher and McDermott, 2007).

CI users are generally provided with limited spectral and temporal information compared to normal hearing listeners (Friesen et al., 2001, Won et al., 2015). The importance of both temporal and spectral resolution for good speech reception has been reported in normal hearing listeners (Xu et al., 2005, Xu and Pfingst, 2008, Souza et al., 2015) and in recipients of auditory prostheses (Shannon, 1992, Cazals et al., 1994, Donaldson and Nelson, 2000, Fu, 2002, 2004, Colletti and Shannon, 2005, Nie et al., 2006). For example, higher speech perception scores are correlated to better temporal processing capabilities, as measured by amplitude modulation detection thresholds (MDTs) (Cazals et al., 1994, Fu, 2002, Won et al., 2011, Gnansia et al., 2014, De Ruiter et al., 2015).

One of the underlying causes for the limited spectral and temporal resolution in CIs could be the large current spread from MP stimulation. Methods to increase the number of truly independent channels available for stimulation and improve spectral resolution by current focusing have become of great interest in CI research. Psychophysical and electrophysiological studies have shown that bipolar (BP) and tripolar (TP) stimulation produce sharper excitation patterns and decreased perceptual interactions among simultaneously stimulated channels compared to MP stimulation (van den Honert and Stypulkowski, 1987, Snyder et al., 1990, Kral et al., 1998, Bierer and Middlebrooks, 2002, 2004, Chatterjee et al., 2006, Srinivasan et al., 2010). However, studies of speech perception have generally shown that CI users tend to perform as well with MP stimulation as with BP and TP stimulation (Zwolan et al., 1996, Pfingst et al., 1997, 2001, Mens and Berenstein, 2005, Berenstein et al., 2008, Fielden et al., 2015). An

electrophysiological study by Middlebrooks (2008b) reported that narrow BP stimulation resulted in higher MDT compared with MP stimulation, suggesting a possible reason for the lack of speech perception benefit with BP stimulation over MP stimulation. Middlebrooks also reported that responses to narrow BP stimuli tended to show increased trial-by-trial variations in first-spike latencies (i.e., temporal jitter) compared to MP stimulation. These results suggest that there may be a link between these two measures of the temporal processing.

Focused multipolar (FMP) stimulation (also referred to as phased array stimulation), has also been used as a method to spatially restrict neural activation in CIs (van den Honert and Kelsall, 2007, Smith et al., 2013, Kalkman et al., 2015, Marozeau et al., 2015). Our previous electrophysiological studies in both acute and long-term deafened animals showed that FMP and TP stimulation can produce a narrower spread of activation in the inferior colliculus (IC) and reduced channel interactions compared to MP stimulation, with no significant differences observed between FMP and TP stimulation (George et al., 2014, 2015a, 2015b). FMP stimulation was also shown to significantly improve subjects' ability to discriminate spectral features and detect dynamic modulations in sound stimuli (Smith et al., 2013). These results indicate that current focusing stimulation (i.e., FMP and TP stimulation) can improve spectral resolution. An important question then arises as to how current focusing stimulation would compare against traditional MP stimulation when conveying amplitude modulation information.

The present study examined IC neural responses to amplitude-modulated electrical pulse trains using FMP and TP stimulation compared to MP stimulation, in acutely deafened guinea pigs. We tested modulation depths from -42 dB (i.e., 0.78% modulation) up to 0 dB (i.e., 100% modulation) and compared responses to unmodulated pulse trains. Measures of modulation sensitivity based on phase locking (vector strengths) and spike count of IC neurons while varying the modulation frequency and stimulus level were compared across stimulation configurations.

METHODS

Experimental Animals

Data were obtained from five young adult pigmented guinea pigs (300 to 600 g) of either sex. All procedures were in accordance with the Australian Code of Practice for the Care and Use of Animals for Scientific Purposes and with the National Institutes of Health, USA guidelines regarding the care and use of animals for experimental procedures, and were approved by the Bionics Institute Animal Research Ethics Committee. The hearing status of each animal was pre-assessed on the day of the experiment by measuring the auditory brainstem response (ABR) to acoustic stimuli delivered to each ear using standard techniques (Coco et al., 2007).

Anaesthesia, Surgery and Recording Procedure

Animals were pre-medicated with atropine sulphate (0.1 mg/kg, intramuscular). Anaesthesia was induced and maintained by administration (via face mask) of isoflurane (3% for induction and 1-1.5% for maintenance) with oxygen (1 L/min). A heating pad was used to maintain the core body temperature at 37.0 ± 1°C. The respiration rate (normal levels: 10-20/min) and end-tidal CO_2 (normal levels: 1-3%) were monitored over the duration of the experiment (15-17 hours).

Prior to the surgery, animals were placed in a stereotaxic frame (David Kopf Instruments, USA). Local anaesthesia using lignocaine (20 mg/mL, subcutaneous) was applied before making an incision above the left pinna. The temporalis muscle was retracted to expose the left tympanic bulla. The bulla was opened, malleoincudal ossicle was removed and the round and oval windows were punctured. The left cochlea was deafened by infusing neomycin sulphate (10% w/v solution) into the round window, and aspirating the solution at the oval window to ensure the access of the drug to all regions of the cochlea (Hardie and Shepherd, 1999). This was done in order to ensure that the electrophysiological responses were not contaminated by electrophonic activity arising from stimulation of hair cells (Black et al., 1983, Sato et al., 2016). Animals were implanted with a Hybrid-L 8 array (HL8), consisting of 8 intracochlear half-band platinum electrodes on a silicon carrier (Shepherd et al., 2011). The electrodes were 0.3 mm in length, spaced ~0.75 mm, centre to centre. The electrode array tapered in diameter from 0.37 to 0.3 mm from the most basal to the most apical electrode. The electrode array was inserted approximately 6.75 mm through the round window into the scala tympani and fixed in place throughout the experiment. Note that the uncoiled length of a guinea pig cochlea is ~18-19 mm (Fernández, 1952) and thus our electrodes were located in mid to high frequency regions.

A craniotomy of the parietal bone was performed on the right dorsolateral portion of the skull and the cerebral cortex was aspirated to expose the IC contralateral to the implanted cochlea. Multi-unit neural activity was recorded using a single shank silicon-substrate recording array (NeuroNexus Technologies, USA) inserted along the cochleotopic axis of the central nucleus of the IC. The array consisted of 32 iridium recording sites spaced at intervals of 100 μm (centre to centre), each having a circular surface area of 413 μm^2. The array was mounted on a microdrive positioner (David Kopf Instruments, USA), positioned at the surface of the IC and advanced ~100 μm s−1 along the dorsolateral to ventromedial extent of the IC, at a 45° angle from the sagittal plane, along the main cochleotopic gradient of the IC (Snyder et al., 1990, Landry et al., 2013). The depth of penetration (~3.5 mm) was chosen by visually monitoring responses of neurons at the tip recording site to electrical stimulation. Multi-unit spike activity from the recording sites was amplified, filtered and digitized at a sampling rate of 30 kHz using a Cerebus data acquisition system (Blackrock Microsystems, USA). At the conclusion of the experiment, the animal was euthanized with an intraperitoneal injection of lethabarb (0.5 mg/kg).

Stimulus Generation and Data Acquisition

Stimulus waveforms were generated by an in-house purpose built multi-channel stimulator, consisting of multiple Howland current sources driven by 12-bit DAC (National Instruments, USA). The stimulator was controlled using custom software implemented in Igor Pro (Wavemetrics, USA). Electrical stimuli consisted of 1 sec modulated/unmodulated trains of biphasic pulses. Individual pulses were charge balanced, cathodic first, 400 μs per phase, with an interphase gap of 50 μs for all tested configurations. A longer phase duration than typically used clinically (25 - 200 μs) was used due to the greater charge required for FMP and TP configurations to evoke neural activity (George et al., 2014). The carrier pulse rate was 120 pps and pulse trains were presented at a repetition rate of 0.5 Hz. While clinical CIs stimulate at higher rates, the carrier pulse rate in this study was limited to 120 pps to ensure that stimulus artefacts did not contaminate the multiunit recordings. The peak amplitude of the stimulus waveform was programmed in clinical current level (CL) units defined by Cochlear Corporation, ranging between 0 and 255, where, current in μA = $17.5 * 100\hat{}(CL/255)$.

Stimuli were presented in MP, TP and FMP stimulation configurations. With MP stimulation, using only one current source, current pulses were delivered to a single intracochlear electrode. With TP stimulation, three current sources were used and current pulses were delivered to a central intracochlear electrode with two adjacent intracochlear electrodes, each carrying half the current in the opposite phase. With FMP stimulation, eight current sources were used to deliver

weighted positive and negative current pulses simultaneously to all intra-cochlear electrodes (van den Honert and Kelsall, 2007, George et al., 2014). Note that FMP stimulation can also be achieved using a single current source (Senn, 2014).

A "channel" in this study refers to a set of cochlear electrodes used to deliver current in a particular stimulation configuration. Channels were numbered increasing from base to apex, in accordance with the convention used in clinical CIs. The number of its centre electrode indicated each FMP and TP channel. For each FMP channel, the weight vector was constructed based on the strategy adapted from van den Honert and Kelsall (2007). A trans-impedance matrix was measured for all intracochlear electrodes, with each column of the inverse of this matrix used to calculate the numerical weights that determined the current from each electrode to produce a single FMP stimulation channel.

A cochlear channel corresponded to one cochlear location in one animal and at that point all three stimulation configurations were tested. Cochlear channels that had at least one adjacent or "flanker" electrode on each side using both FMP and TP were stimulated with unmodulated and modulated pulse trains using FMP, TP and MP stimulation. Amplitude modulated stimuli were sinusoidal modulated pulse trains (figure 1). Pulse trains were modulated by the function

$$1 + \frac{m\cos\left(2\pi f_m(t)\right)}{2} - \frac{m}{2}$$

where m is the modulation depth (defined as the ratio between the minimum and peak current levels, adapted from (Perry, 2012)) and f_m is the modulation frequency (in Hz). Modulation frequencies used were 10, 20, 30 and 40 Hz. Modulation depths when represented in decibels as $20\log_{10}(m)$ ranged from 0 to -42 dB in 6 dB steps (i.e., 100, 50, 25, 12.5, 6.25, 3.125, 1.5625, 0.78125 and 0% modulation; figure 1). The peak current level of the modulated/unmodulated pulse train was fixed at 2 dB above the threshold of the unmodulated pulse train. A subset of CI channels were also tested at 1 and 4 dB above the threshold. Combinations of stimulation configuration, modulation frequency, modulation depth and peak current level were presented at random with each repeated 5 times.

Data Analysis

Single- and multi-unit recordings were processed offline, using customized spike detection scripts in IgorPro (Wavemetrics, USA). The signal was band-pass filtered (0.3-5 kHz) and stimulus artefacts were removed using techniques detailed in Heffer and Fallon (2008). Spikes were detected when the signal exceeded four times root mean square for each recording channel (Fallon et al., 2009). Analysis was performed on a 50 to 1050 ms window after onset of the

pulse train (figure 1); responses prior to 50 ms were excluded to avoid any effects that may have occurred due to the onset of the stimulus. For each stimulus condition, spike counts were averaged across five trials and normalized between the spontaneous activity rate (average rate in 33–3 ms pre-stimulus window) and maximum response across stimulation configurations on a particular recording site as detailed in Landry et al., (2013). Thresholds were estimated from "IC response images" in which normalized spike rates were displayed with the stimulus intensity on the y-axis and the depth of the recording site on the x-axis (figure 3); this analysis is detailed in our previous study (George et al., 2014). The lowest current that elicited a normalized spike rate of 0.3 using an unmodulated pulse train was defined as the IC threshold (Landry et al., 2013) for each cochlear channel. A minimum of 0.3 was chosen for threshold so that spike rates on the best recording site and those adjacent to it were higher than 2 s.d. of the mean spontaneous rate. IC threshold and the best recording site (i.e., the recording site that yielded the lowest threshold) were computed for each CI channel when presented with unmodulated pulse trains. We also calculated the first spike latency and the standard deviation of the first spike latency across trials (i.e., temporal jitter) for each best recording site.

<Figure 1 about here>

Figure 1: Electrical stimulus waveforms and IC neural responses. Amplitude vs. time plots of a) an unmodulated biphasic pulse train, and pulse trains modulated at b) -12 dB and c) 0 dB. Individual pulses were charge balanced, cathodic-first, 400 μs per phase, with an interphase gap of 50 μs (shown in the inset in (a)). Carrier pulse rate was 120 pps, modulation frequency was 10 Hz and the stimulus duration was 1 sec. Panels d-f) Traces of multi-unit responses (including 200 ms pre-stimulus) from a recording site in the IC following electrical stimulation of a CI channel using FMP stimulation at the modulation depths shown in panels a-c. Each panel of spike responses demonstrate locking to the envelope of the stimulus depicted in the panel above. Dotted lines indicate the start of the stimulus. Data presented here are after stimulus artefact removal. Panels g-i) Peri-stimulus time histogram (binwidth=8.3 ms) for the responses to unmodulated and modulated pulse trains (shown in the panel above) including pre-stimulus activity. Analysis was performed after excluding responses between 0-50 ms post stimulus (shown in shaded rectangle). Panels j-k) Modulation cycle histograms (binwidth = $\pi/6$) generated from the spike responses across five trials of the stimuli shown in panels a-c, demonstrating the extent of phase locking of IC spike activity. The mean vector strength (VS) computed for different modulation depths are indicated in the corresponding panel.

IC neural responses to a modulated stimuli were characterized by a) averaged spike rate across the duration of stimulation and b) the vector strength of IC neuronal phase locking at the modulation frequency. The extent of phase locking of IC spikes to the modulator waveform was quantified by computing the vector strength (Goldberg and Brown, 1969, Middlebrooks, 2008a, Krishna and Semple, 2000). Vector strength was calculated only for trials that resulted in activity of more than four spikes over the 1s recording period to avoid erroneously high vector strengths for channels without very good driven activity (Middlebrooks, 2008b). Each spike was expressed as a unit vector, with the phase (θ) obtained by expressing the spike time relative to the stimulus period. The mean vector strength was determined by averaging the resulting vector (across n spikes over the duration of stimulation). Vector strength could vary from a minimum of 0 (no phase locking) to a maximum of 1 (all spikes occur at the same unique phase). The statistical significance of the vector strength was assessed by applying the Rayleigh's test of circular uniformity at the level of $p < 0.01$ (Stephens, 1969).

The change in vector strength with modulation depth (figure 2a, b) at each recording site was quantified by the discrimination index, d', computed by a procedure derived from signal detection theory (Green and Swets, 1966, Macmillan and Creelman, 2005). A receiver operator characteristic curve was formed based on vector strengths elicited for five trials when the stimulus was modulated and unmodulated, by varying the vector strength criterion from 0 to 1. The area under the receiver operator characteristic curve was expressed as a standard deviate and the resulting z-score was multiplied by $\sqrt{2}$ to obtain d'. For the best recording site (i.e., the recording site that was most sensitive to a particular stimulation configuration) of each stimulating channel, the value of d' was computed across modulation depths of -42 to 0 dB, in steps of 6 dB. The lowest interpolated modulation depth that yielded a d' of 1 was chosen as the MDT (figure 2c, d), an adaption of the methodology described by Middlebrooks (2008b).

Additionally, for all best recording sites in the IC, plots of average spike rate across five trials (in the 50 to 1050 ms window after the onset of the pulse train) versus stimulation level (rate-level curves) were generated using responses to unmodulated pulse trains. From these plots, the slopes around 1, 2 and 4 dB above the threshold (i.e., the increase in spike rate from 5 CL below to 5 CL above) were computed and compared across the different stimulation configurations. This was done in order to assess if the rate-level curve would be related to the modulation sensitivity for different stimulation configurations.

<Figure 2 about here>

Figure 2: Overview of the calculation of modulation detection thresholds (MDTs). a, b) Vector strength (mean ± SEM) versus modulation depth plots are shown for FMP, TP and MP stimulation configurations demonstrating the trend of vector strength with modulation depth of a) multi-unit activity from an individual IC site and b) a single-unit (shown inset), across five trials. The vector strength computed for unmodulated stimulation in each configuration is also shown. c, d) Values of d' are plotted as a function of modulation depth corresponding to the panel above for the 3 stimulation configurations. Each value of d' was computed from the area of the receiver operator characteristics curve formed based on vector strengths calculated for five trials when the stimulus was unmodulated and modulated at a particular depth. The modulation depth when each interpolated plot crosses d' of 1 was chosen as the MDT (arrows in c and d). The modulated and unmodulated pulse trains are presented at 2 dB above the threshold of an unmodulated pulse train.

Statistical Analysis

All statistical analyses were performed using SigmaPlot Version 13.5 (Systat, USA). The data were pooled over all stimulated channels. Comparisons of IC threshold, spike rate and temporal jitter between MP, TP and FMP stimulation were performed using one-way RM ANOVAs, with Tukey corrected post-hoc testing of individual comparisons where appropriate. A two-way RM ANOVA was performed to compare the effects of two stimulus parameters on MDTs. Simple linear regression was used as a measure of correlation between two variables.

RESULTS

Across five animals, we tested four cochlear channels each in four animals and one cochlear channel in the final animal, thus totalling 17 cochlear channels. We obtained measurements of IC neural responses from 160 recording sites based on five recording array placements. We extracted 10 single units, which showed similar pattern of responses as the multiunit activity (as shown in figure 2). However, due to the limited number, these units were not analysed further separately. The main analyses were done on multiunit activity from the 17 best recording sites (i.e., the recording site that was most sensitive to each CI channel). The best recording sites for FMP, TP and MP stimulation of a particular CI channel were not always the same, as observed in our previous studies.

IC response images were generated for electrical stimulation with MP, FMP and TP stimulation configurations using unmodulated pulse trains. Figure 3 illustrates IC response images and the spatial tuning curves (STCs) from one animal following electrical stimulation of cochlear channel 6 (in the apical third of the array) using the three different stimulation configurations. STCs were generated for each response image (shown by the white line) by joining the stimulus intensities that yielded a normalized spike rate of 0.3 on each recording site. Consistent with our previous results in cats (George et al., 2014, 2015b), the width of the STC increased with increasing stimulus intensity above threshold. MP stimulation resulted in very broad STCs, generally spreading across the entire recording array and resulting in significant myogenic activity at higher intensities while FMP and TP STCs were similarly narrow at low intensities."

<*Figure 3 about here*>

Figure 3: Response images across the cochleotopic axis of the IC to electrical stimulation using unmodulated pulse train in a) FMP b) TP and c) MP stimulation configurations in an acutely-deafened guinea pig. Each response image was labelled according to configuration and channel number (shown for stimulating channel 6). The tip of each response image corresponded to the recording site that is most sensitive to that particular stimulation configuration.

Average Spike Rate

For each cochlear channel, the spike rate in the 50 to 1050 ms window after the onset of the pulse train was derived for the best recording site. There was a monotonic increase in spike rate with increasing stimulation level found in the rate-level curves (figure 4a). Consistent with our previous animal studies using single pulses (George et al., 2014, 2015b), thresholds for IC activation using single pulses and unmodulated pulse trains were significantly higher (one-way RM ANOVAs, $p < 0.001$) for FMP and TP than for the MP configuration. Using single pulses, IC thresholds averaged 37.6 ± 3.4 dB (re 1 μA; mean ± SEM) for MP, 50.3 ± 7.2 dB for FMP and 51.9 ± 8.2 dB for TP stimulation. IC thresholds using unmodulated pulse trains averaged 40.1 ± 4.6 dB (re 1 μA; mean ± SEM) for MP, 52.7 ± 8.7 dB for FMP and 53.8 ± 8.5 dB for TP stimulation. A paired *t*-test confirmed no significant difference between IC thresholds using single pulse and unmodulated pulse train ($p > 0.05$).

We analysed the slope of the rate-level curve for the unmodulated pulse train around 1, 2 and 4 dB above the threshold for a subset of channels (n=12). Around 1 and 2 dB above the threshold, the rate-level slope was significantly dependent on stimulation configuration (figure 4b; one-way RM ANOVA, $p < 0.05$), with FMP and TP stimulation having a significantly shallower slope compared to MP stimulation. However, no significant difference was observed between

stimulation configurations around 4 dB above the threshold. To determine the effect of stimulation level on the rate-level slope for each stimulation configuration, independent one-way RM ANOVAs were performed. With FMP and TP stimulation, no significant difference was observed between slopes measured at different stimulation levels. However, MP rate-level slopes were shallower around 4 dB than at 1 and 2 dB above the threshold (p-values < 0.05).

<Figure 4 about here>

Figure 4: a) Mean spike rate (mean ± SEM) across five trials versus stimulation level function of the best recording site for an unmodulated pulse presented in different stimulation configurations. Threshold level and levels of 2 and 4 dB above the threshold are indicated (filled symbols). b) Group mean (mean ± SEM) for rate-level slope (i.e., the change in spike rate in 10 CL) for MP, TP and FMP stimulation configurations for different stimulation levels tested. * $p < 0.05$. n=12 recording sites

Figure 5 shows the mean spike rate measured for FMP (circles), TP (triangles) and MP (squares) stimulation as a function of modulation depth for various modulation frequencies. Note that the mean spike rate measured for stimulation using an unmodulated pulse train is also shown in each plot.

<Figure 5 about here>

Figure 5: Spike rate (mean ± SEM) in the 50 to 1050 ms window after the onset of the pulse train, plotted as a function of modulation depth for various stimulation configurations. Each panel represent a particular modulation frequency, as indicated. Spike rate corresponding to the unmodulated pulse train is also included in each panel. The modulated and unmodulated pulse trains are presented at 2 dB above the threshold of an unmodulated pulse train. n =17 recording sites.

We observed a general trend of reduction in the overall spike rate with increased modulation depths. In the case of MP stimulation, a significant reduction in the spike rate was observed from -18 dB onwards (compared to the unmodulated stimulus) at all modulation frequencies (one-way RM ANOVA, $p < 0.05$). For FMP and TP stimulation, spike rate was significantly reduced at -6 dB and at 0 dB (one-way RM ANOVA, $p < 0.05$).

Cycle Histograms

Modulation cycle histograms, which show the distribution of spikes over the phase of the modulating waveform, demonstrated the temporal patterning of IC activity across various stimulation configurations and various modulation depths (figure 6). In each panel, the associated vector strength, which quantifies the phase locked firing of spikes i.e., the tendency of spikes to occur over a range of phases of the stimulating waveform, is indicated. The top row of panels shows the spike patterns to unmodulated pulse trains and lower values of vector strength indicate the absence of/weaker phase locking. For all stimulation configurations, phase locking was weak at very low modulation depths, and strengthened with increasing with modulation depth.

<Figure 6 about here>

Figure 6: Modulation cycle histograms of spikes across five trials measured at the best recording site to electrical stimulation of a CI channel in FMP, TP and MP stimulation configurations. Each column of panels show responses to pulse trains sinusoidally modulated at 10 Hz and at various depths, as indicated. The modulated/unmodulated pulse trains were presented at 2dB above the threshold of the unmodulated pulse train**.** Spike times occurring 50 to 1050 ms after onset of the pulse train are binned according to modulator phase, $\pi/6$. Total spike rate (TSR) and

vector strength (VS; averaged across five trials) are indicated in each panel. * indicates significant vector strength (Rayleigh's test; $p < 0.01$). Note that the best recording site of each stimulation configuration was different.

Peak spike rate

In contrast to the mean spike rate, the peak spike rate (i.e. the maximum of the cycle histogram) showed an increasing trend with increased modulation depths with all three stimulation configurations (Figure 6). This is because the spikes get clustered more tightly so the peak rate increases as vector strength increases while the mean spike rate decreases as shown in figure 5. These data are summarised in Figure 7 and demonstrated that MP stimulation showed a significant increase in peak spike rate (compared to the unmodulated stimulus) when using depth of -12 dB and onwards, while FMP and TP stimulation only showed a significant increase when using a depth of 0 dB (one-way RM ANOVAs, p-values < 0.05). We did not observe a change in the best modulation phase across different stimulation configurations, stimulation channels or modulation frequencies.

<Figure 7 about here>

Figure 7: Mean spike rate at the peak of the cycle histogram plotted as a function of modulation depth for various stimulation configurations. Spike rate corresponding to the unmodulated pulse train is also included. The modulated pulse trains were presented at 2dB above the threshold of an unmodulated pulse train and were modulated at 10 Hz. n =17 recording sites.

Vector Strength

The distributions of vector strength across all best recording sites for FMP, TP and MP stimulation configurations, and for modulation frequencies of 10, 20, 30 and 40 Hz are shown in figure 8. These distributions include vector strengths of best recording sites from all animals, represented by different symbols, with closed symbols representing vector strengths that were statistically significant (Rayleigh test, $p < 0.01$) and open symbols indicating vector strengths that were not significant. The vector strengths computed for IC responses to unmodulated pulse trains presented in three different stimulation configurations are also shown (dotted lines). In every panel, vector strengths increased monotonically with increasing modulation depth. Vector

strengths varied amongst stimulation configurations, with 50% of sites showing significant vector strengths with MP stimulation at modulation depths greater than or equal to -24 dB, and with FMP and TP stimulation at modulation depths greater than or equal to -12 dB.

In order to assure that artefact contamination did not affect our vector strengths (as artefacts could vary between stimulation configurations), we implemented additional measures in the analyses that included analysis of single unit activity (figure 2b), and analyses of recording sites away from the best recording site (which would have the same artefacts and background noise but different spiking activity). These distant recording sites did not exhibit any significant vector strengths regardless of the configuration, confirming that the phase locking observed on the best recording sites were indeed from spiking activity, and not from stimulus artefacts.

<Figure 8 about here>

Figure 8: Columns 1-3) Distribution of vector strengths across the best recording sites from all the animals. Each row represents vector strengths for modulation frequencies of 10, 20, 30 and 40 Hz and columns represent various stimulation configurations, as indicated. Each individual animal's data are represented with a different symbol. Every vector strength is shown, with closed symbols indicating statistically significant vector strengths ($p < 0.01$, Rayleigh test) and open symbols indicating those that failed to produce significant phase locking. In each panel, dotted lines indicate the average vector strength computed across the best recording sites when stimulated with unmodulated pulse trains in a particular stimulation configuration. The modulated pulse trains are presented at 2dB above the threshold of an unmodulated pulse train**.** Column 4) Mean vector strength (mean ± SEM) versus modulation depth across different stimulation configurations. n=17 recording sites across 5 animals.

Modulation Detection Threshold

Figure 9 shows MDTs based on vector strength for the best recording sites to electrical stimulation of cochlear channels in different stimulation configurations. A two-way RM ANOVA (stimulation configuration and modulation frequency as factors) showed that MDTs were significantly different between stimulation configurations ($p < 0.001$) and not between different modulation frequencies ($p > 0.05$), with no significant interaction between stimulation configuration and modulation frequency ($p > 0.05$). Post-hoc tests indicated that MP stimulation exhibited lower MDTs than FMP and TP stimulation (p-values < 0.001), and no significant difference was observed between FMP and TP stimulation ($p > 0.05$). The MDTs measured across all modulation frequencies averaged -18.08 ± 0.87 dB for FMP, -17.62 ± 0.82 dB for TP and -26.47 ± 1.08 dB for MP stimulation.

<Figure 9 about here>

Figure 9: Modulation transfer functions (i.e., MDT (mean ± SEM) versus modulation frequency (Hz)) based on vector strength of the best recording sites shown for FMP (circle), TP (triangle) and MP (square) stimulation configurations. The modulated pulse trains are presented at 2 dB above the threshold of an unmodulated pulse train. n=17 recording sites across 5 animals.

Temporal Jitter

An independent measure of the temporal characteristics of responses to each stimulation configuration was provided by the first spike latency and temporal jitter calculated as the standard deviation of first spike latency. Both first spike latency and temporal jitter generally decreased monotonically with increasing current level. At 2 dB above the threshold, the first spike latency ranged from 3.8 ms to 5.9 ms across all three stimulation configurations, with mean value of 4.78 ± 0.34 ms for FMP, 4.70 ± 0.29 ms for TP and 4.55 ± 0.13 ms for MP stimulation. The jitter values measured at 2 dB above threshold averaged 0.73 ± 0.35 ms, 0.69 ± 0.29 ms and 0.54 ± 0.26 ms for FMP, TP and MP stimulation respectively. Both the first spike latency and the temporal jitter did not differ significantly between different stimulation configurations (one-way RM ANOVA, $p > 0.05$, n=17).

Effect of stimulation level on MDT

To study the effects of overall stimulation level on MDTs, a subset of CI channels (9 channels across 3 animals) were stimulated at lower (1 dB above the threshold) and higher (4 dB above the threshold) stimulation levels. At l dB above the threshold, configuration effects on MDTs was similar to that observed at 2 dB above the threshold i.e., MP stimulation exhibited lower MDTs than FMP and TP stimulation (figure 10; one-way RM ANOVA, p-values < 0.01) with no significant difference between FMP and TP stimulation ($p > 0.05$). However, at 4 dB above the threshold, no significant difference was observed between the different stimulation configurations (figure 10; one-way RM ANOVA, p-values > 0.05).

<Figure 10 about here>

Figure 10: Group means (mean ± SEM) for modulation detection thresholds for MP, TP and FMP stimulation configurations for different stimulation levels tested. * $p < 0.01$, ** $p < 0.001$. n=17 recording sites for 2 dB and n=9 recording sites for 1 and 4 dB

To determine the effect of stimulation level on MDTs for each stimulation configuration, independent one-way RM ANOVAs were performed. In the case of MP stimulation, MDTs measured at higher stimulation level (i.e., at 4 dB) were significantly higher than that measured

at lower stimulation levels (p-values < 0.05). With FMP and TP stimulation, no significant difference was observed between MDTs measured at different stimulation levels.

Effect of stimulation site on MDT

The modulation sensitivity or the strength of phase locking varied according to the site of the CI channel. Figure 11 shows the distribution of MDTs as a function of CI channel number measured across all modulation frequencies for different stimulation configurations. For each stimulation configuration, MDTs exhibited a significant correlation with the stimulation site (p-values < 0.001). Highest MDTs were recorded for the basal CI channels. This dependency is likely to be the major factor contributing to the wide variations observed in vector strengths in figure 8. However, we didn't observe significant apical/basal differences of other parameters such as first spike latency and spike rate.

<Figure 11 about here>

Figure 11: Distribution of MDTs as a function of CI channel for various stimulation configurations. Data is shown for channels stimulated with modulated pulse trains with peak current at 2 dB above the threshold. Data across all tested modulation frequencies is grouped together.

DISCUSSION

In the present study, we evaluated the responses of IC neurons to sinusoidal amplitude-modulated pulse trains using FMP and TP stimulation, and compared these to responses obtained with MP stimulation. We also examined the effects of stimulation level and modulation frequency on modulation sensitivity for the different stimulation configurations. The sensitivity of IC neurons to amplitude modulation was characterized based on the average spike rate over the duration of the stimulus and the strength of phase locking, represented by the vector strength. To the best of our knowledge, the data presented in this paper represents the first report of electrophysiological modulation detection using FMP and TP stimulation.

The main finding of this study was that at lower stimulation levels (1 and 2 dB above threshold), MP stimulation had lower MDTs than FMP or TP stimulation, while no significant difference was observed between FMP and TP stimulation. However, at 4 dB above threshold MDTs did not differ significantly between stimulation configurations, as a result of increased MDTs at higher stimulation levels with MP stimulation. Moreover, we observed a reduction in spike rate with increased modulation depths, with MP stimulation resulting in a significant reduction in spike rate at shallower modulation depths than FMP and TP stimulation. We did not observe any difference between different modulation frequencies tested. Finally, modulation sensitivity was generally poorer when stimulating more basal CI channels.

It is worth noting that in the present study comparisons of stimulation configuration at particular stimulation levels expressed in dB re threshold may be confounded by the fact that we might have operated at different levels of dynamic range given the previous reports of different dynamic ranges for MP, TP and FMP (George et al., 2014, 2015b). For example, 2 dB above the threshold might be at different loudness level i.e., a softer level for FMP and TP stimulation compared to MP stimulation (see top panel of figure 4, where MP stimulation resulted in higher spike rates compared to FMP and TP stimulation). However, given that MDTs were similar across all stimulation levels (i.e., 1, 2 and 4 dB above threshold) for FMP and TP stimulation, this difference in dynamic range between the stimulation configurations should not affect the main findings.

Relation to other animal studies

The present study can be compared with the electrophysiological study conducted by Middlebrooks (2008b) in acutely deafened guinea pigs. That study examined phase locking of neurons in the auditory cortex to the envelope of modulated pulse trains presented in MP and narrow BP (i.e., adjacent active and return electrodes) stimulation configurations, with both

683 configurations using the next-to-most apical intra-cochlear electrode as the active electrode.
684 Middlebrooks reported that modulation detection of MP stimulation was significantly better
685 than narrow BP stimulation for the 254 and 4096 pps carrier rates. Similarly, for the 120 pps
686 carrier rate, the present study showed that MP stimulation tended to have enhanced modulation
687 sensitivity compared to FMP and TP stimulation. However, the advantage in modulation
688 sensitivity with MP over FMP and TP stimulation was only observed at low stimulation levels.
689 This may be in part explained by the steeper rate-level slopes found when using MP stimulation
690 with unmodulated pulse trains (figure 4) resulting in a larger change in spike rate across the
691 modulation cycle. This in turn would have led to a sharper cycle histogram (figure 6) and hence
692 a higher vector strength. However, at higher stimulus levels, we observed that MP rate-level
693 curves were flatter around 4 dB than at 2 dB above threshold, while the slopes for focused
694 stimulation were unchanged, which might account for the decrease in modulation sensitivity of
695 MP stimulation at higher stimulation levels.

696 Even though the stimulation levels in Middlebrooks' study were set to 2, 4 and 6 dB above
697 threshold, data was reported only for the stimulation level that produced the lowest MDT when
698 comparing MP with BP stimulation. Therefore, it is possible that a similar level effect may have
699 been present in the Middlebrooks study but it was not evident due to the collapsing across
700 stimulation level. Middlebrooks proposed that the better modulation sensitivity seen with MP
701 stimulation was due to the widespread and synchronous neural activation that typically occurs
702 with MP stimulation. This hypothesis was supported by the significantly lower temporal jitter
703 observed in response to MP stimulation compared to BP stimulation. In contrast, there was no
704 significant difference in temporal jitter at 2 dB above threshold in the present study between all
705 three stimulation configurations tested. We observed that IC neurons exhibited mean first spike
706 latencies in the range 3.8 to 5.9 ms across all three stimulation configurations, consistent with
707 previous reports from our lab using similar experimental techniques (Landry et al., 2013). While
708 the present study observed a reduction in IC spike rate with increased modulation depth,
709 Middlebrooks' study reported that the spike rate typically increased with modulation depth. The
710 discrepancy between these two results is likely to be related to differences in the modulation
711 waveforms used. The present study used modulated waveforms with the peak amplitude fixed
712 (i.e., maximum down modulation); thereby, greater modulation depths resulting in reduced
713 number of points where current level exceeds neural threshold (refer figure 1c). In contrast, the
714 Middlebrooks' study used modulated waveforms with current levels ranging above and below
715 (i.e., mean up and down modulation) the mean current in modulated waveform, such that the
716 peak amplitude increased with increase in modulation depth and typically resulting in increased

717 spike rates. Finally, Middlebrooks' data showed a considerable increase in the percentage of
718 units that showed no phase locking at any modulation depth with BP stimulation. This effect
719 was, however, not evident with TP or FMP stimulation in the present study. A likely
720 explanation for the failure to find this effect is that the present study analysed only the best
721 recording sites or the most sensitive units while Middlebrooks reported every unit that was
722 recorded. Moreover, some of the differences found between the two studies might be a
723 consequence of the difference in recording structure i.e., IC versus auditory cortex. These
724 structures are known to have different limiting rate, which is much higher in the IC i.e., ~120 Hz
725 (Middlebrooks and Snyder, 2010) than auditory cortex i.e., ~20 Hz (Fallon et al., 2014).
726 Notably, in the present study, even though we excluded responses prior to 50 ms to avoid onset
727 response, we observed that 100% of best recording sites displayed a significant time locked
728 response (vector strength ranging from 0.46 to 0.99 upon including first 50 ms and 0.48 to 0.99
729 upon excluding response prior to 50 ms) to each pulse in the carrier pulse train employed at 120
730 pps for all stimulation configurations and all stimulation sites. Finally, there are also differences
731 in the level of spectral integration that occurs in the IC and auditory cortex (Irvine, 1992,
732 Casseday et al., 2002, Read et al., 2002), which may contribute to some of the differences
733 between the present study and Middlebrooks' study.

734 *Relation to human studies*

735 The ability to detect amplitude modulation has been widely used to measure the temporal-
736 envelope processing capability in CI users. Modulation transfer functions, defined as the plot of
737 MDTs as a function of modulation frequency, measured in CI subjects generally show low pass
738 characteristics with a 100-150 Hz cut-off frequency (Shannon, 1992, Busby et al., 1993).
739 Similarly, for the low modulation rates used in this study (10 – 40 Hz), there was no change in
740 the modulation sensitivity with modulation frequencies.

741 Consistent with several reports on the significant variability in MDTs across listeners and also
742 across stimulation sites within listeners (Fu, 2002, Colletti and Shannon, 2005, Pfingst et al.,
743 2008, Garadat et al., 2012), we observed that vector strengths and MDTs varied widely among
744 stimulation sites for all stimulation configurations. There have been reports of systematic
745 variation in MDTs along the cochlear length in some CI users (Pfingst et al., 2007, 2011,
746 Garadat et al., 2012). Consistent with these reports, the present study showed a clear tendency
747 for more apical channels to have enhanced modulation sensitivity. This could be related to the
748 systematic anatomical differences along the cochlear spiral, such as wider cross-sectional
749 diameter of the scala at more basal locations, resulting in current to flow along different
750 pathways. It is also possible that these variations could be induced by differences in the location

of the stimulating electrodes relative to the modiolus as a function of cochlear length. There is a dramatic decrease of cross sectional area after 4-5 mm in the guinea pig cochlea from ~1.1-1.3mm to ~0.3-0.4mm (Fernández, 1952, Wada et al., 1998, Thorne et al., 1999) hence the most apical contacts were likely to be located very close to the modiolar wall. The present result is also consistent with the results of the study by Middlebrooks and Snyder (2010) in which they showed that low frequency IC sites had better temporal acuity than high frequency sites. In the present study, the correlation between MDTs and stimulation site was similar for the broad MP stimulation and the focused stimulation (i.e., FMP and TP). This is attributed to our analysis that was based only on the best recording sites rather than the whole recording array.

There are several caveats to note when comparing the present animal study with human psychophysical data. Among these are a range of species-dependent factors and differences in the experimental methodology including duration of deafness and electrical stimulation parameters. Additionally, MDTs determined using psychophysical approaches may differ methodologically from the electrophysiologically determined MDTs in the midbrain described in the present study. Stimulation levels in human psychophysical studies are normally set at levels within the dynamic range from threshold to most comfortable level whereas, the present study tested modulation sensitivity at stimulation levels relative to the lowest IC activation threshold. Most human psychophysical studies have found that MDTs generally improve as the stimulation level is increased (though some CI users were reported to show no effect above 30% of their dynamic range (Shannon, 1992, Fu, 2002, Galvin and Fu, 2009)). In contrast, we observed that modulation sensitivity of MP stimulation reduced at higher stimulation levels. A similar trend of decrease in modulation sensitivity with increased stimulation level was reported by Middlebrooks (2008b). In 77.7% cases of MP stimulation and 24.6% and 22.5% cases of FMP and TP respectively, we observed that IC neurons were driven to saturation at 4 dB above threshold. This might have contributed to the impairment of modulation sensitivity of MP stimulation at high stimulation levels. However, modulation sensitivities of FMP and TP stimulation showed no stimulation level effect, demonstrating the adequate modulation detection capability of FMP and TP stimulation even at high stimulation levels. Moreover, FMP and TP stimulation were found to have similar modulation sensitivity. This is consistent with our previous electrophysiological studies that showed similar performance in spatial selectivity and channel interactions with FMP and TP stimulation (George et al., 2014, 2015a, 2015b).

One of the limitations of the present study is that the carrier rate was limited to 120 pps, lower than typically used clinically i.e., 250 to ~ 4,000 pps, to ensure that stimulus artefacts did not contaminate the multi-unit recordings. Middlebrooks (2008b) reported a systematic decrease in

the modulation sensitivity with increasing carrier rate. However, the result of BP stimulation producing a significant decrease in modulation sensitivity compared with MP stimulation was observed at both low and high carrier rates in that study. Based on these reports by Middlebrooks, it is expected that the differences we observed between FMP, TP and MP stimulation at the low carrier rate used in this study will be maintained when using a higher carrier rate. Pfingst et al., (2007) found that in addition to higher MDTs for a 4,000 pps carrier rate compared to a 250 pps carrier rate, there was a significant interaction between carrier rate and stimulation site with lower modulation sensitivity at the apical stimulation site observed when using the higher carrier rate. Therefore, it is also possible that the apical/basal differences found in our study would be different when using a higher carrier rate.

In summary, the results from the present study demonstrated elevated MDTs using FMP and TP stimulation, compared to MP stimulation, at low stimulation levels. However, the current focusing techniques such as FMP and TP stimulation remain capable of conveying amplitude modulation at high stimulation levels, at least within the confines of the present study, which to our knowledge has not been demonstrated previously. Previous results from our laboratory have shown significant improvements in spatial selectivity as well as reduced channel interactions with FMP and TP stimulation compared to MP stimulation, even in cochleae with significant neural degeneration. Associating the present data to our previous studies highlights the possible trade-off between spectral and temporal fidelity with these current focusing techniques. The exact phenomenon that limits the modulation sensitivity of more restricted stimulation techniques is still not clear. Future work needs to be done to explore the mechanism by which phase locking to focused stimulation might impair transmission of modulating waveforms. In addition, it would be interesting to see if speech perception using FMP and TP would be different in take-home CI experiments with more complex listening tasks, such as listening to speech in background noise.

Acknowledgement

This study was funded by The Garnett Passe and Rodney Williams Memorial Foundation, the ARC (LP 48 130 100 220) and the NHMRC. SSG was supported by an Australian Postgraduate Award through the Australian Government and the Bartholomew Reardon PhD Scholarship through the Bionics Institute. The Bionics Institute acknowledges the support it receives from the Victorian Government through its Operational Infrastructure Support Program. We thank Dr. Philipp Senn for multi-channel stimulator engineering and support, Helen Feng for electrode manufacture and Dr. Sue Pierce for veterinary advice.

821 REFERENCES

822

823 BERENSTEIN, C. K., MENS, L. H., MULDER, J. J. & VANPOUCKE, F. J. 2008. Current steering and
824 current focusing in cochlear implants: comparison of monopolar, tripolar, and virtual channel electrode
825 configurations. *Ear Hear,* 29**,** 250-60.
826 BIERER, J. A. & MIDDLEBROOKS, J. C. 2002. Auditory cortical images of cochlear-implant stimuli:
827 dependence on electrode configuration. *J. Neurophysiol,* 87**,** 478-92.
828 BIERER, J. A. & MIDDLEBROOKS, J. C. 2004. Cortical responses to cochlear implant stimulation:
829 channel interactions. *J. Assoc. Res. Otolaryngol,* 5**,** 32-48.
830 BLACK, R. C., CLARK, G. M., O'LEARY, S. J. & WALTERS, C. 1983. Intracochlear electrical
831 stimulation of normal and deaf cats investigated using brainstem response audiometry. *Acta*
832 *Otolaryngol Suppl,* 399**,** 5-17.
833 BUSBY, P. A., TONG, Y. C. & CLARK, G. M. 1993. The perception of temporal modulations by
834 cochlear implant patients. *J. Acoust. Soc. Am,* 94**,** 124-31.
835 CASSEDAY, J. H., FREMOUW, T. & COVEY, E. 2002. The inferior colliculus: a hub for the central
836 auditory system. *Integrative functions in the mammalian auditory pathway.* New York: Springer.
837 CAZALS, Y., PELIZZONE, M., SAUDAN, O. & BOEX, C. 1994. Low-pass filtering in amplitude
838 modulation detection associated with vowel and consonant identification in subjects with
839 cochlear implants. *J. Acoust. Soc. Am,* 96**,** 2048-54.
840 CHATTERJEE, M., GALVIN, J. J., 3RD, FU, Q. J. & SHANNON, R. V. 2006. Effects of stimulation
841 mode, level and location on forward-masked excitation patterns in cochlear implant patients. *J.*
842 *Assoc. Res. Otolaryngol,* 7**,** 15-25.
843 COCO, A., EPP, S. B., FALLON, J. B., XU, J., MILLARD, R. E. & SHEPHERD, R. K. 2007. Does
844 cochlear implantation and electrical stimulation affect residual hair cells and spiral ganglion
845 neurons? *Hear. Res,* 225**,** 60-70.
846 COLLETTI, V. & SHANNON, R. V. 2005. Open set speech perception with auditory brainstem
847 implant? *The Laryngoscope,* 115**,** 1974-1978.
848 DE RUITER, A. M., DEBRUYNE, J. A., CHENAULT, M. N., FRANCART, T. & BROKX, J. P. 2015.
849 Amplitude Modulation Detection and Speech Recognition in Late-Implanted Prelingually and
850 Postlingually Deafened Cochlear Implant Users. *Ear Hear,* 36**,** 557-66.
851 DONALDSON, G. S. & NELSON, D. A. 2000. Place-pitch sensitivity and its relation to consonant
852 recognition by cochlear implant listeners using the MPEAK and SPEAK speech processing
853 strategies. *J. Acoust. Soc. Am,* 107**,** 1645-58.
854 DORMAN, M. F. 1993. Speech perception by adults. *In:* TYLER, R. S. (ed.) *Cochlear implants:*
855 *Audiological foundations.* San Diego: Singular Publishing Group Inc.
856 FALLON, J. B., IRVINE, D. R. & SHEPHERD, R. K. 2009. Cochlear implant use following neonatal
857 deafness influences the cochleotopic organization of the primary auditory cortex in cats. *J.*
858 *Comp. Neurol,* 512**,** 101-14.
859 FERNÁNDEZ, C. 1952. Dimensions of the cochlea (guinea pig). *The Journal of the Acoustical Society*
860 *of America,* 24**,** 519-523.
861 FIELDEN, C. A., KLUK, K., BOYLE, P. J. & MCKAY, C. M. 2015. The perception of complex pitch in
862 cochlear implants: A comparison of monopolar and tripolar stimulation. *J. Acoust. Soc. Am,* 138**,**
863 2524.
864 FRIESEN, L. M., SHANNON, R. V., BASKENT, D. & WANG, X. 2001. Speech recognition in noise as
865 a function of the number of spectral channels: comparison of acoustic hearing and cochlear
866 implants. *J. Acoust. Soc. Am,* 110**,** 1150-63.
867 FU, Q.-J. 2002. Temporal processing and speech recognition in cochlear implant users. *Neuroreport,* 13**,**
868 1635-1639.
869 FU, Q. J., SHANNON, R. V. & WANG, X. 1998. Effects of noise and spectral resolution on vowel and
870 consonant recognition: acoustic and electric hearing. *J. Acoust. Soc. Am,* 104**,** 3586-96.
871 FU, Q. J., CHINCHILLA, S. & GALVIN, J. J. 2004. The role of spectral and temporal cues in voice
872 gender discrimination by normal-hearing listeners and cochlear implant users. *J. Assoc. Res.*
873 *Otolaryngol,* 5**,** 253-60.
874 GALVIN, J. J., 3RD & FU, Q. J. 2009. Influence of stimulation rate and loudness growth on modulation
875 detection and intensity discrimination in cochlear implant users. *Hear. Res,* 250**,** 46-54.

GARADAT, S. N., ZWOLAN, T. A. & PFINGST, B. E. 2012. Across-site patterns of modulation detection: relation to speech recognition. *J. Acoust. Soc. Am,* 131**,** 4030-41.

GEORGE, S. S., WISE, A. K., SHIVDASANI, M. N., SHEPHERD, R. K. & FALLON, J. B. 2014. Evaluation of focused multipolar stimulation for cochlear implants in acutely deafened cats. *J. Neural Eng,* 11**,** 065003.

GEORGE, S. S., SHIVDASANI, M. N., WISE, A. K., SHEPHERD, R. K. & FALLON, J. B. 2015a. Electrophysiological channel interactions using focused multipolar stimulation for cochlear implants. *J. Neural Eng,* 12**,** 066005.

GEORGE, S. S., WISE, A. K., FALLON, J. B. & SHEPHERD, R. K. 2015b. Evaluation of focused multipolar stimulation for cochlear implants in long-term deafened cats. *J. Neural Eng,* 12**,** 036003.

GNANSIA, D., LAZARD, D. S., LEGER, A. C., FUGAIN, C., LANCELIN, D., MEYER, B. & LORENZI, C. 2014. Role of slow temporal modulations in speech identification for cochlear implant users. *Int J Audiol,* 53**,** 48-54.

GOLDBERG, J. M. & BROWN, P. B. 1969. Response of binaural neurons of dog superior olivary complex to dichotic tonal stimuli: some physiological mechanisms of sound localization. *J. Neurophysiol,* 32**,** 613-36.

GREEN, D. M. & SWETS, J. A. 1966. *Signal detection theory and psychophysics*, Wiley New York.

HARDIE, N. A. & SHEPHERD, R. K. 1999. Sensorineural hearing loss during development: morphological and physiological response of the cochlea and auditory brainstem. *Hear. Res,* 128**,** 147-65.

HEFFER, L. F. & FALLON, J. B. 2008. A novel stimulus artifact removal technique for high-rate electrical stimulation. *J. Neurosci. Meth,* 170**,** 277-84.

IRVINE, D. R. 1992. Physiology of the auditory brainstem. *The mammalian auditory pathway: Neurophysiology*. New York: Springer

KALKMAN, R. K., BRIAIRE, J. J. & FRIJNS, J. H. 2015. Current focusing in cochlear implants: An analysis of neural recruitment in a computational model. *Hear. Res,* 322**,** 89-98.

KRAL, A., HARTMANN, R., MORTAZAVI, D. & KLINKE, R. 1998. Spatial resolution of cochlear implants: the electrical field and excitation of auditory afferents. *Hear. Res,* 121**,** 11-28.

KRISHNA, B. S. & SEMPLE, M. N. 2000. Auditory temporal processing: responses to sinusoidally amplitude-modulated tones in the inferior colliculus. *J. Neurophysiol,* 84**,** 255-273.

LANDRY, T. G., FALLON, J. B., WISE, A. K. & SHEPHERD, R. K. 2013. Chronic neurotrophin delivery promotes ectopic neurite growth from the spiral ganglion of deafened cochleae without compromising the spatial selectivity of cochlear implants. *J. Comp. Neurol,* 521**,** 2818-32.

MACMILLAN, N. A. & CREELMAN, C. D. 2005. *Detection theory: A user's guide,* New Jersy, Lawrence Erlbaum.

MAROZEAU, J., MCDERMOTT, H. J., SWANSON, B. A. & MCKAY, C. M. 2015. Perceptual interactions between electrodes using focused and monopolar cochlear stimulation. *J. Assoc. Res. Otolaryngol,* 16**,** 401-12.

MCDERMOTT, H. J., MCKAY, C. M. & VANDALI, A. E. 1992. A new portable sound processor for the University of Melbourne/Nucleus Limited multielectrode cochlear implant. *J. Acoust. Soc. Am,* 91**,** 3367-71.

MENS, L. H. & BERENSTEIN, C. K. 2005. Speech perception with mono- and quadrupolar electrode configurations: a crossover study. *Otol. Neurotol,* 26**,** 957-64.

MIDDLEBROOKS, J. C. 2008a. Auditory cortex phase locking to amplitude-modulated cochlear implant pulse trains. *J. Neurophysiol,* 100**,** 76-91.

MIDDLEBROOKS, J. C. 2008b. Cochlear-implant high pulse rate and narrow electrode configuration impair transmission of temporal information to the auditory cortex. *J. Neurophysiol,* 100**,** 92-107.

MIDDLEBROOKS, J. C. & SNYDER, R. L. 2010. Selective electrical stimulation of the auditory nerve activates a pathway specialized for high temporal acuity. *The Journal of Neuroscience,* 30**,** 1937-1946.

NIE, K., BARCO, A. & ZENG, F. G. 2006. Spectral and temporal cues in cochlear implant speech perception. *Ear Hear,* 27**,** 208-17.

PERRY, D. W. 2012. *Temporal Processing in the Deafened Auditory Cortex.* PhD Thesis, The University of Melbourne.

PFINGST, B. E., ZWOLAN, T. A. & HOLLOWAY, L. A. 1997. Effects of stimulus configuration on psychophysical operating levels and on speech recognition with cochlear implants. *Hear. Res,* 112**,** 247-260.

PFINGST, B. E., FRANCK, K. H., XU, L., BAUER, E. M. & ZWOLAN, T. A. 2001. Effects of electrode configuration and place of stimulation on speech perception with cochlear prostheses. *J. Assoc. Res. Otolaryngol,* 2**,** 87-103.

PFINGST, B. E., XU, L. & THOMPSON, C. S. 2007. Effects of carrier pulse rate and stimulation site on modulation detection by subjects with cochlear implants. *J Acoust Soc Am,* 121**,** 2236-46.

PFINGST, B. E., BURKHOLDER-JUHASZ, R. A., XU, L. & THOMPSON, C. S. 2008. Across-site patterns of modulation detection in listeners with cochlear implants. *J. Acoust. Soc. Am,* 123**,** 1054-62.

PFINGST, B. E. 2011. Effects of electrode configuration on cochlear implant modulation detection thresholds. *The Journal of the Acoustical Society of America,* 129**,** 3908-3915.

READ, H. L., WINER, J. A. & SCHREINER, C. E. 2002. Functional architecture of auditory cortex. *Curr Opin Neurobiol,* 12**,** 433-40.

SATO, M., BAUMHOFF, P. & KRAL, A. 2016. Cochlear Implant Stimulation of a Hearing Ear Generates Separate Electrophonic and Electroneural Responses. *J Neurosci,* 36**,** 54-64.

SENN, P. 2014. *Peripheral nerve stimulation for the treatment of chronic neuropathic pain.* PhD, University of Melbourne.

SHANNON, R. V. 1992. Temporal modulation transfer functions in patients with cochlear implants. *J Acoust Soc Am,* 91**,** 2156-64.

SHEPHERD, R., VERHOEVEN, K., XU, J., RISI, F., FALLON, J. & WISE, A. 2011. An improved cochlear implant electrode array for use in experimental studies. *Hear. Res,* 277**,** 20-27.

SKINNER, M. W., CLARK, G. M., WHITFORD, L. A., SELIGMAN, P. M., STALLER, S. J., SHIPP, D. B., SHALLOP, J. K., EVERINGHAM, C., MENAPACE, C. M. & ARNDT, P. L. 1994. Evaluation of a new spectral peak coding strategy for the Nucleus 22 channel cochlear implant system. *Otol. Neurotol,* 15**,** 15-27.

SMITH, Z. M., PARKINSON, W. S. & LONG, C. J. Multipolar current focusing increases spectral resolution in cochlear implants. 35th Annual International Conf. of the IEEE Engineering in Medicine and Biology Society, 2013. 2796-99.

SNYDER, R. L., REBSCHER, S. J., CAO, K. L., LEAKE, P. A. & KELLY, K. 1990. Chronic intracochlear electrical stimulation in the neonatally deafened cat. I: Expansion of central representation. *Hear. Res,* 50**,** 7-33.

SOUZA, P. E., WRIGHT, R. A., BLACKBURN, M. C., TATMAN, R. & GALLUN, F. J. 2015. Individual sensitivity to spectral and temporal cues in listeners with hearing impairment. *J Speech Lang Hear Res,* 58**,** 520-34.

SRINIVASAN, A. G., LANDSBERGER, D. M. & SHANNON, R. V. 2010. Current focusing sharpens local peaks of excitation in cochlear implant stimulation. *Hear. Res,* 270**,** 89-100.

STEPHENS, M. 1969. Tests for randomness of directions against two circular alternatives. *Journal of the American Statistical Association,* 64**,** 280-289.

SUCHER, C. M. & MCDERMOTT, H. J. 2007. Pitch ranking of complex tones by normally hearing subjects and cochlear implant users. *Hear. Res,* 230**,** 80-7.

THORNE, M., SALT, A. N., DEMOTT, J. E., HENSON, M. M., HENSON, O. W., JR. & GEWALT, S. L. 1999. Cochlear fluid space dimensions for six species derived from reconstructions of three-dimensional magnetic resonance images. *Laryngoscope,* 109**,** 1661-8.

VAN DEN HONERT, C. & STYPULKOWSKI, P. H. 1987. Single fiber mapping of spatial excitation patterns in the electrically stimulated auditory nerve. *Hear. Res,* 29**,** 195-206.

VAN DEN HONERT, C. & KELSALL, D. C. 2007. Focused intracochlear electric stimulation with phased array channels. *J. Acoust. Soc. Am,* 121**,** 3703-16.

WADA, H., SUGAWARA, M., KOBAYASHI, T., HOZAWA, K. & TAKASAKA, T. 1998. Measurement of guinea pig basilar membrane using computer-aided three-dimensional reconstruction system. *Hear Res,* 120**,** 1-6.

WILSON, B. S., FINLEY, C. C., LAWSON, D. T., WOLFORD, R. D., EDDINGTON, D. K. & RABINOWITZ, W. M. 1991. Better speech recognition with cochlear implants. *Nature,* 352**,** 236-238.

WON, J. H., DRENNAN, W. R., NIE, K., JAMEYSON, E. M. & RUBINSTEIN, J. T. 2011. Acoustic temporal modulation detection and speech perception in cochlear implant listeners. *J. Acoust. Soc. Am,* 130**,** 376-88.

WON, J. H., MOON, I. J., JIN, S., PARK, H., WOO, J., CHO, Y. S., CHUNG, W. H. & HONG, S. H. 2015. Spectrotemporal Modulation Detection and Speech Perception by Cochlear Implant Users. *PLoS One,* 10**,** e0140920.

XU, L., THOMPSON, C. S. & PFINGST, B. E. 2005. Relative contributions of spectral and temporal cues for phoneme recognition. *J. Acoust. Soc. Am,* 117**,** 3255-67.

XU, L. & PFINGST, B. E. 2008. Spectral and temporal cues for speech recognition: implications for auditory prostheses. *Hear. Res,* 242**,** 132-40.

ZWOLAN, T. A., KILENY, P. R., ASHBAUGH, C. & TELIAN, S. A. 1996. Patient performance with the Cochlear Corporation" 20+ 2" implant: bipolar versus monopolar activation. *Otol. Neurotol,* 17**,** 717-23.

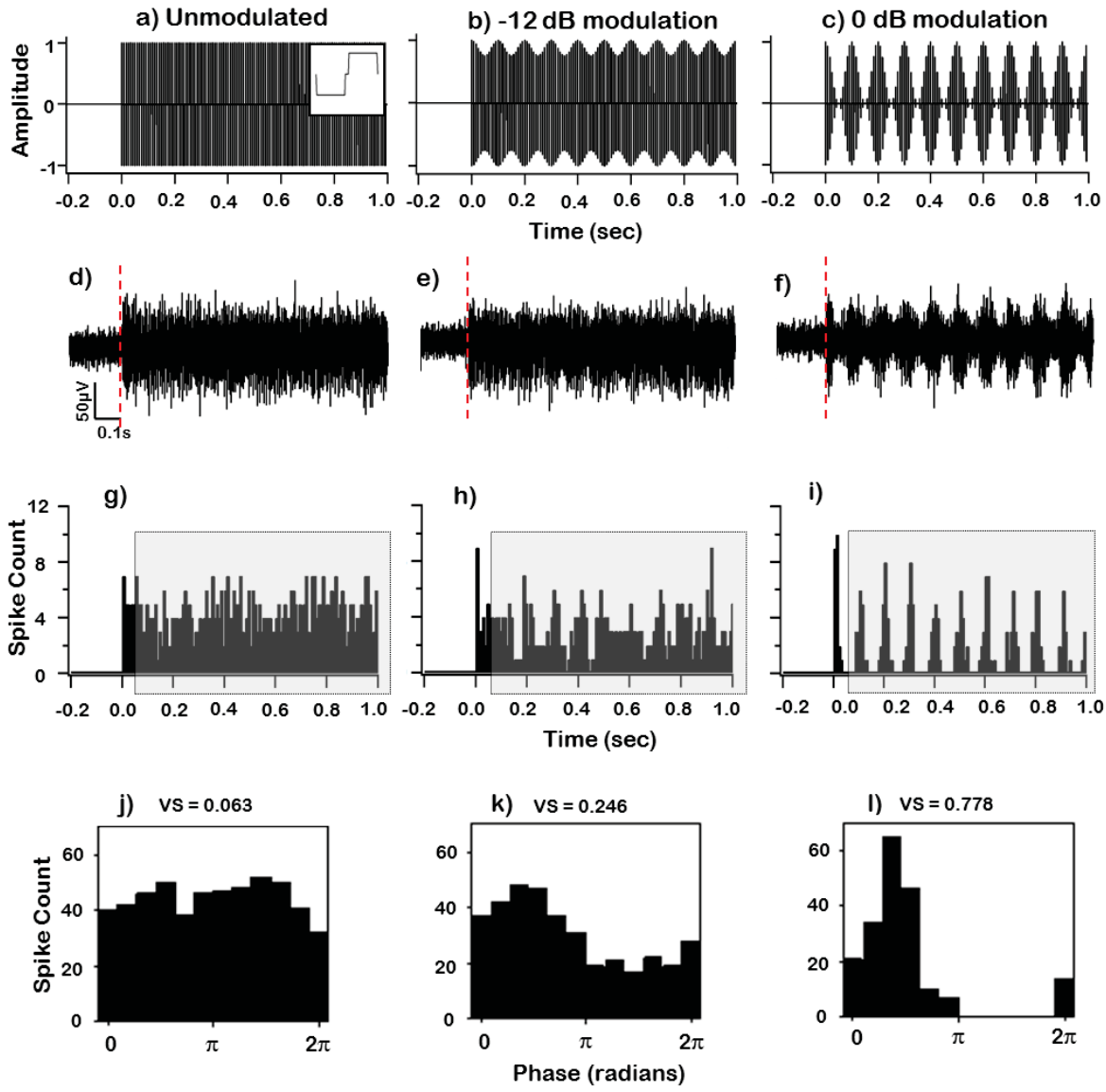
a) Unmodulated
b) -12 dB modulation
c) 0 dB modulation
Amplitude
Time (sec)
d)
e)
f)
50μV
0.1s
g)
h)
i)
Spike Count
Time (sec)
j) VS = 0.063
k) VS = 0.246
l) VS = 0.778
Spike Count
Phase (radians)

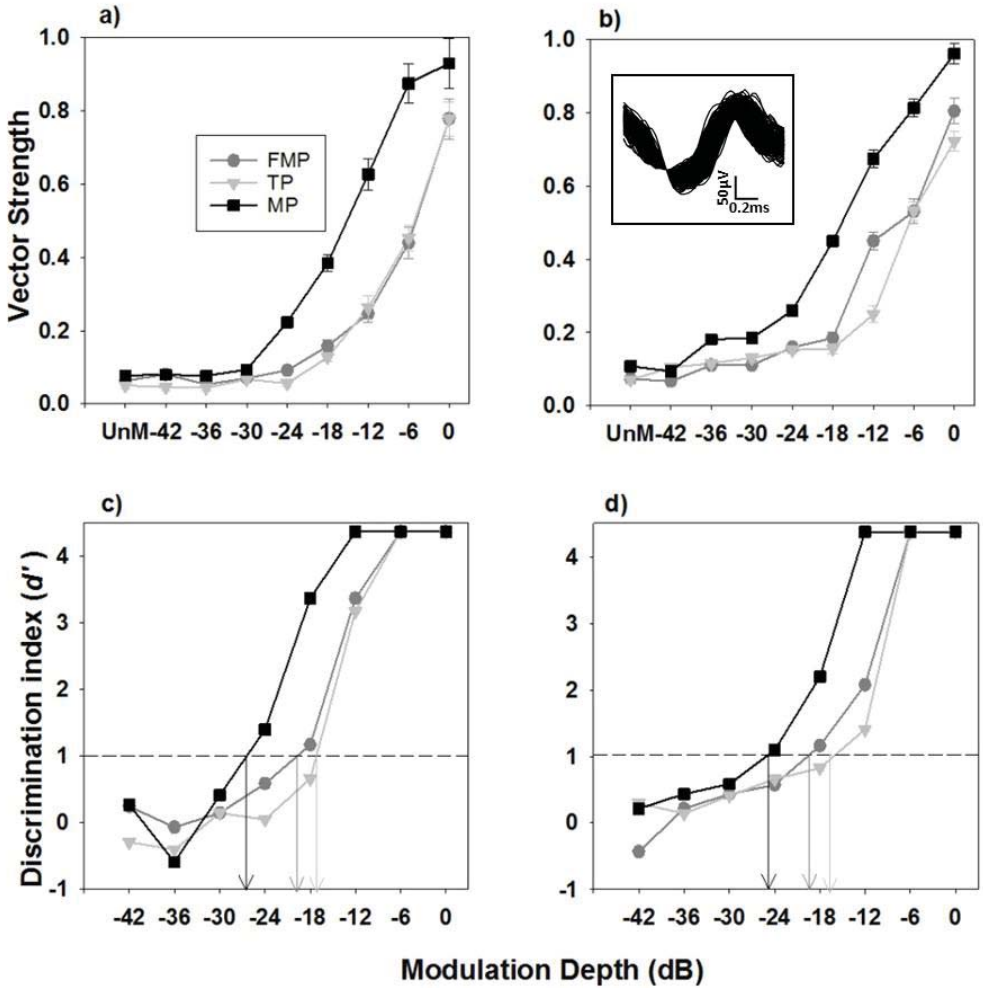
a)
b)
c)
d)
Vector Strength
Discrimination index (d')
Modulation Depth (dB)
FMP
TP
MP
UnM -42 -36 -30 -24 -18 -12 -6 0
50µV
0.2ms

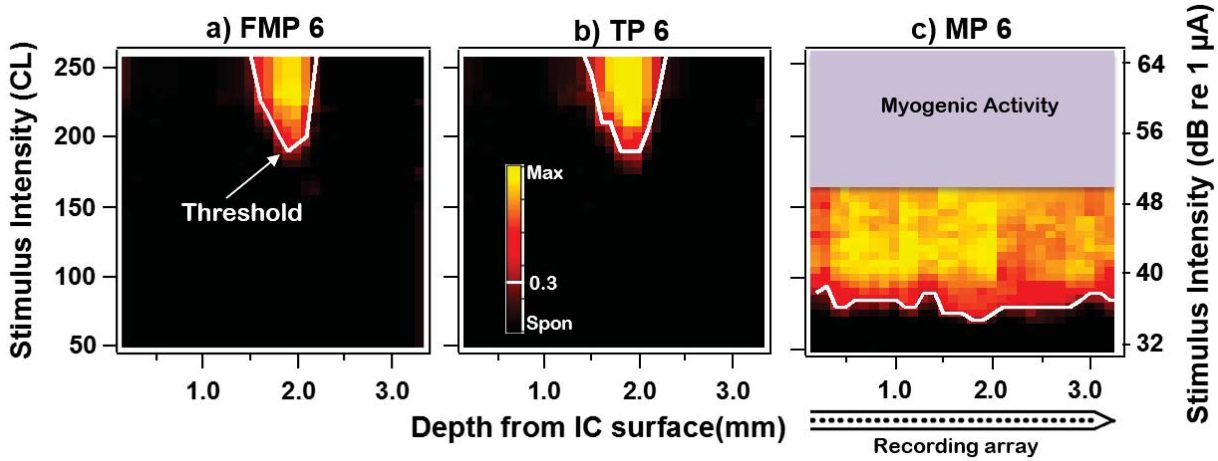
a) FMP 6
b) TP 6
c) MP 6
Stimulus Intensity (CL)
250
200
150
100
50
Threshold
Max
0.3
Spon
Myogenic Activity
64
56
48
40
32
Stimulus Intensity (dB re 1 µA)
1.0
2.0
3.0
Depth from IC surface(mm)
Recording array

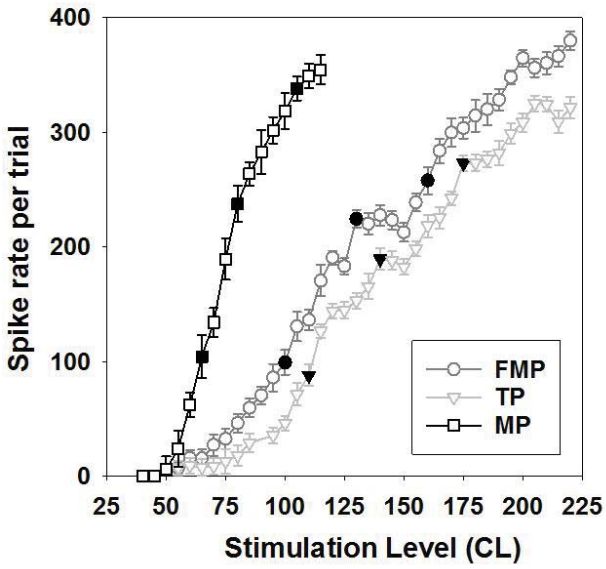
Spike rate per trial
400
300
200
100
0
25
50
75
100
125
150
175
200
225
Stimulation Level (CL)
FMP
TP
MP

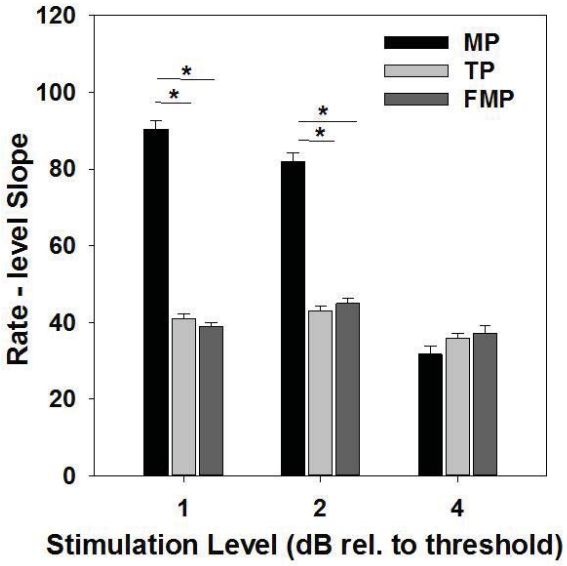
Rate - level Slope
120
100
80
60
40
20
0
MP
TP
FMP
*
*
*
*
1
2
4
Stimulation Level (dB rel. to threshold)

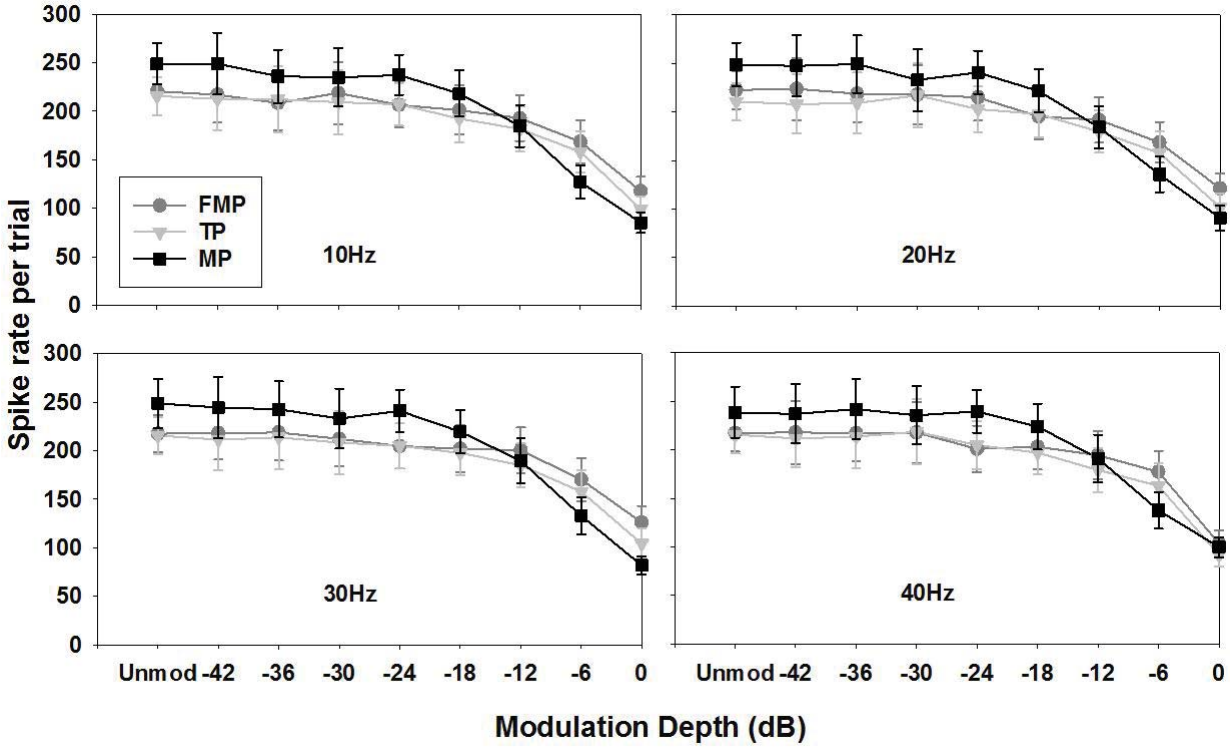
Spike rate per trial
300
250
200
150
100
50
0
FMP
TP
MP
10Hz
20Hz
30Hz
40Hz
Unmod
-42
-36
-30
-24
-18
-12
-6
0
Modulation Depth (dB)

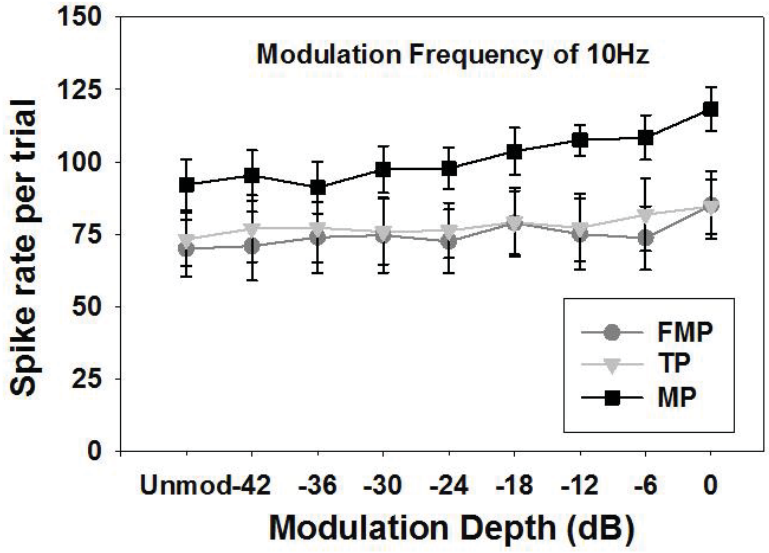
Modulation Frequency of 10Hz
Spike rate per trial
150
125
100
75
50
25
0
Unmod
-42
-36
-30
-24
-18
-12
-6
0
Modulation Depth (dB)
FMP
TP
MP

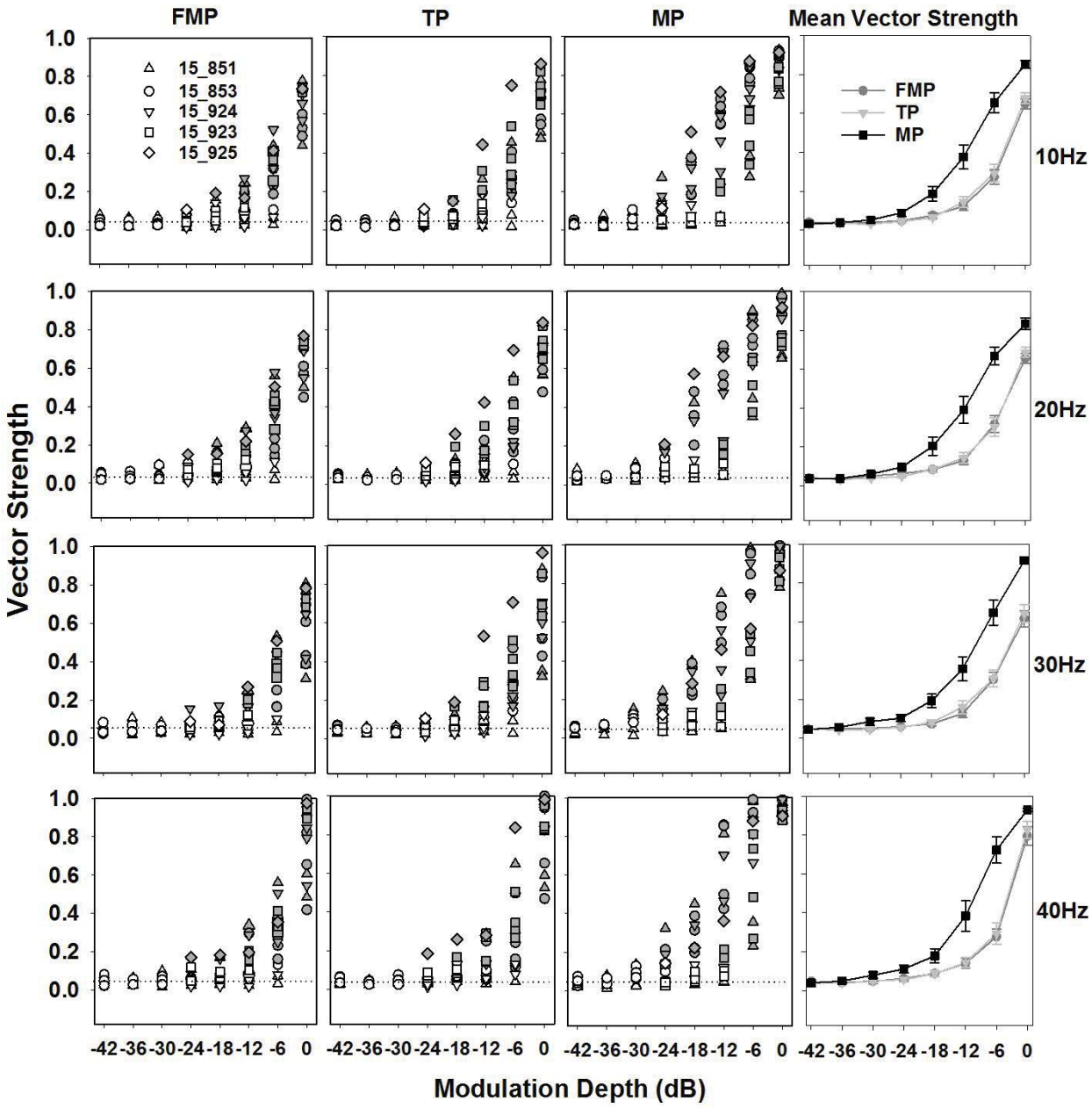
FMP
TP
MP
Mean Vector Strength
15_851
15_853
15_924
15_923
15_925
FMP
TP
MP
10Hz
20Hz
30Hz
40Hz
Vector Strength
1.0
0.8
0.6
0.4
0.2
0.0
-42 -36 -30 -24 -18 -12 -6 0
Modulation Depth (dB)

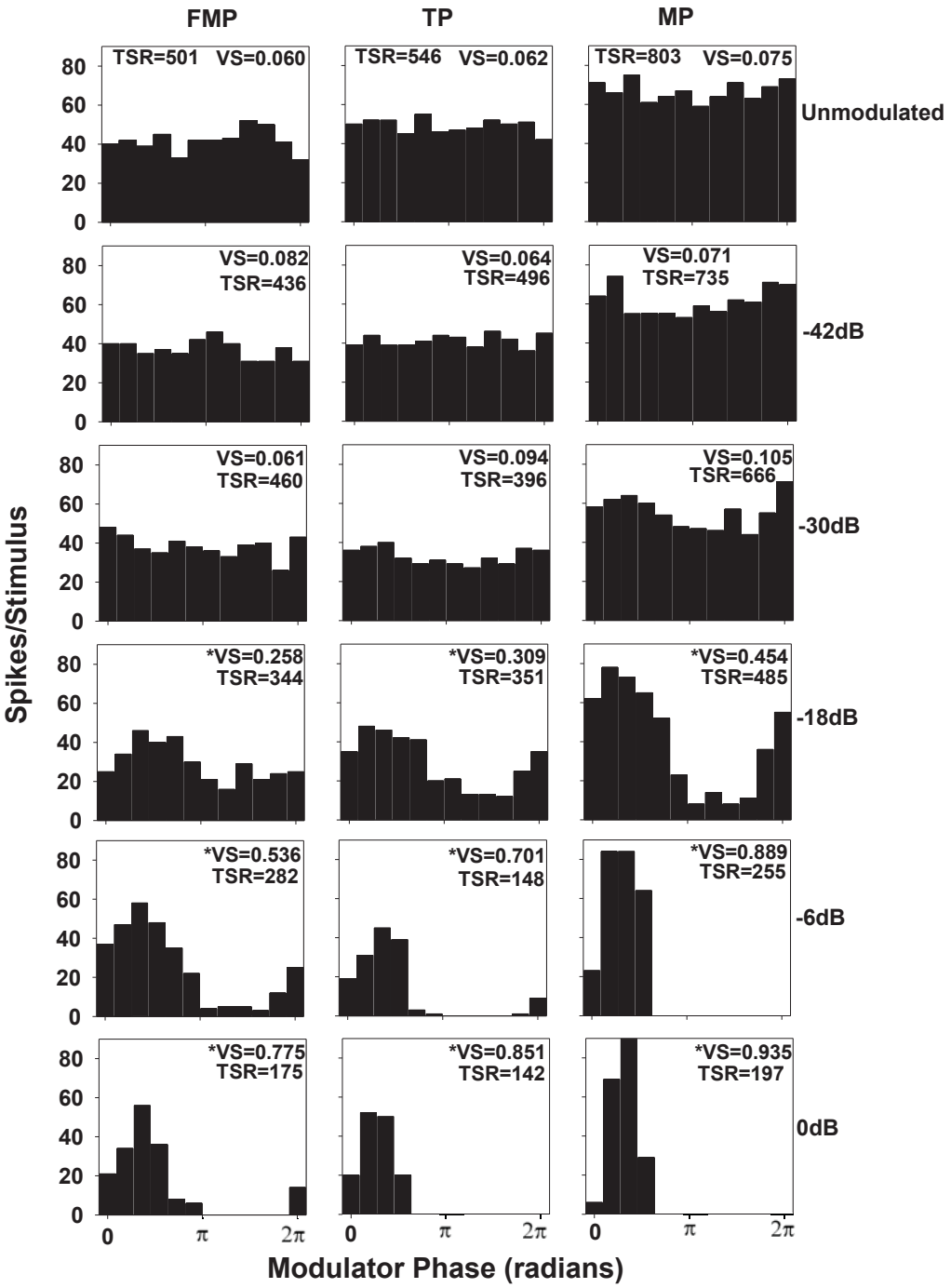
FMP
TP
MP
TSR=501 VS=0.060
TSR=546 VS=0.062
TSR=803 VS=0.075
Unmodulated
VS=0.082
TSR=436
VS=0.064
TSR=496
VS=0.071
TSR=735
-42dB
VS=0.061
TSR=460
VS=0.094
TSR=396
VS=0.105
TSR=666
-30dB
*VS=0.258
TSR=344
*VS=0.309
TSR=351
*VS=0.454
TSR=485
-18dB
*VS=0.536
TSR=282
*VS=0.701
TSR=148
*VS=0.889
TSR=255
-6dB
*VS=0.775
TSR=175
*VS=0.851
TSR=142
*VS=0.935
TSR=197
0dB
Spikes/Stimulus
0
20
40
60
80
0
π
2π
Modulator Phase (radians)

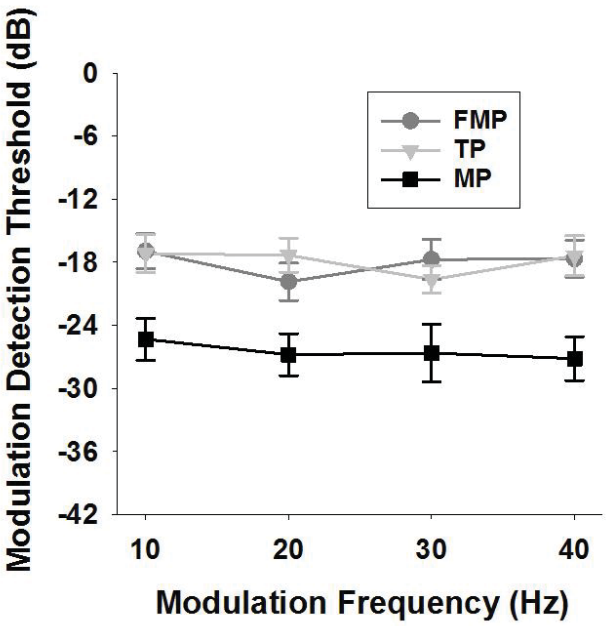
Modulation Detection Threshold (dB)
0
-6
-12
-18
-24
-30
-36
-42
10
20
30
40
Modulation Frequency (Hz)
FMP
TP
MP

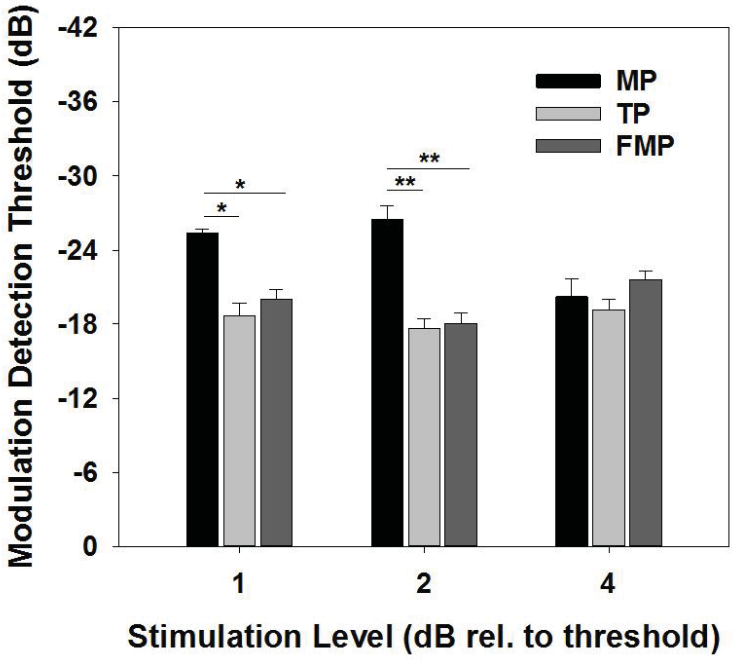
Modulation Detection Threshold (dB)
-42
-36
-30
-24
-18
-12
-6
0
MP
TP
FMP
*
*
**
**
1
2
4
Stimulation Level (dB rel. to threshold)

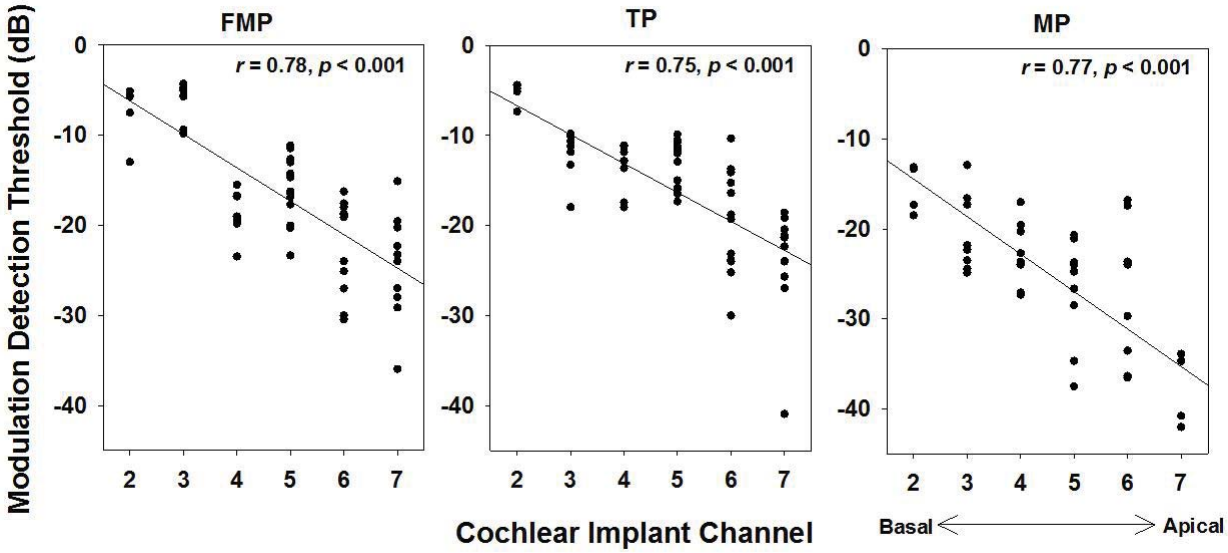
FMP
TP
MP
r = 0.78, p < 0.001
r = 0.75, p < 0.001
r = 0.77, p < 0.001
Modulation Detection Threshold (dB)
0
-10
-20
-30
-40
2
3
4
5
6
7
Cochlear Implant Channel
Basal
Apical